Synthesis and Properties of Monomer Casting Polyamide 6/Poly(methyl methacrylate) Blends

Tongfei Wu,[1,2] Tingxiu Xie,[3] Guisheng Yang[1,3]

[1]*Key Laboratory of Engineering Plastics, Joint Laboratory of Polymer Science and Technology, Institute of Chemistry, Chinese Academy of Sciences, Beijing 100080, People's Republic of China*
[2]*Graduate University, Chinese Academy of Sciences, Beijing 100039, People's Republic of China*
[3]*Shanghai Genius Advanced Materials Company, Limited, Shanghai 201109, People's Republic of China*

Received 4 January 2008; accepted 29 July 2008
DOI 10.1002/app.29014
Published online 26 September 2008 in Wiley InterScience (www.interscience.wiley.com).

ABSTRACT: We successfully synthesized monomer casting polyamide 6 (MCPA6)/poly(methyl methacrylate) (PMMA) blends in two steps: (1) radical polymerization of methyl methacrylate in ε-caprolactam and (2) anionic ring-opening polymerization of this ε-caprolactam solution. The influence of PMMA on the crystallization behavior of MCPA6 was studied with differential scanning calorimetry and X-ray diffraction, which showed that PMMA could act as a heterogeneous nucleation agent and favored the formation of the γ-crystalline form. The rheological properties were also studied and indicated that PMMA reduced the interaction between MCPA6 chains by lowering the density of hydrogen bonding. This study used a novel and convenient method to prepare microporous MCPA6/PMMA particles that involved removing the continuous phase. Their surface area and thermal stability were characterized by the Brunauer–Emmett–Teller method and thermogravimetric analysis, respectively. © 2008 Wiley Periodicals, Inc. J Appl Polym Sci 111: 101–107, 2009

Key words: blends; compatibility; crystallization

INTRODUCTION

Poly(methyl methacrylate) (PMMA) and other polyacrylates are polymers with ester linkages on the side chains. The difficulty of synthesizing monomer casting polyamide 6 (MCPA6)/PMMA blends by the anionic ring-opening polymerization of ε-caprolactam (CLA) is the activating activity of the ester linkage on its side chains needed to form the graft polymer.

As is well known, lots of esters can act as activators of the anionic ring-opening polymerization of CLA, such as γ-butyrolactone[1,2] and ε-caprolactone,[3–5] which have been reported. In fact, almost all esters that can be dissolved in CLA can activate the anionic ring-opening polymerization of CLA. We performed this anionic ring-opening polymerization activated by methyl methacrylate and butyl methacrylate at 95°C in our laboratory. We confirmed that they have enormous activating activity. In addition to these small-molecule activators, polyesters also can act as activators of the anionic ring-opening polymerization of CLA: aliphatic esters, such as poly(ε-caprolactone),[6] poly(lactic acid), and poly(γ-butyrolactone), and aromatic esters, such as poly(ethylene terephthalate), poly(butylene terephthalate), polycarbonate, and thermoplastic poly(ether urethane) elastomer,[7] which has ester linkages on its molecular chains. However, not all of these activators have equivalent activating activity. The lowest temperatures at which the anionic ring-opening polymerization of CLA can be activated are about 90, 130, 150, and 180°C for poly(ε-caprolactone),[6] polycarbonate, poly(ethylene terephthalate) or poly(butylene terephthalate), and thermoplastic poly(ether urethane) elastomer,[7] respectively. The lowest temperature depends on the solubility of the polyester in CLA. The mechanism is that an ester reacts with a CLA sodium salt, which produces one *N*-acetylcaprolactam (*N*-COCLA) and one alcohol sodium salt.[6] *N*-COCLA is the activator of the anionic ring-opening polymerization of CLA.

Fortunately, we have confirmed that PMMA has a faint activity for activating the anionic ring-opening polymerization of CLA, and this faint activity could almost be ignored in this study because the period of blend synthesis is short enough. In this work, we synthesized MCPA6/PMMA blends with PMMA contents varying from 0.5 to 10 wt %. The influence of PMMA on the crystallization behavior of MCPA6 was also studied with differential scanning calorimetry (DSC) and X-ray diffraction (XRD). The rheological properties of MCPA6/PMMA blends were investigated. We also used a novel and convenient method to prepare microporous MCPA6/PMMA particles. Their surface area and thermal stability were characterized by the Brunauer–Emmett–Teller

Correspondence to: G. Yang (ygs@geniuscn.com).

(BET) method and thermogravimetric analysis (TGA), respectively.

EXPERIMENTAL

Materials

CLA was obtained from Grodno Joint Stock Co. (Grodno, Republic of Belarus). Methyl methacrylate, 2,2′-azobisisobutyronitrile (AIBN) used as an initiator for acrylic polymerization, NaOH, and *N*-COCLA used as an activator in this work were purchased from Shanghai Chemical Reagents Co. (Shanghai, China) and used without further treatment.

Synthesis of PMMA in CLA

PMMA was synthesized from methyl methacrylate by radical polymerization in CLA. A mixture of MMA (20 g), AIBN (0.2 g), and CLA (80 g) was placed in a 250-mL glass flask and heated at 80°C for 10 h with tender mechanical stirring. The resulting solution was used to prepare MCPA6/PMMA blends. Some PMMA was precipitated into water and purified by extraction with hot water to measure the molecular weight by gel permeation chromatography (number-average molecular weight = 8600 g/mol, polydispersity index = 2.1).

Synthesis of the MCPA6/PMMA blends

A certain amount of a PMMA solution was diluted to the desired concentration with CLA. The resulting mixture was kept *in vacuo* at 140°C for 20 min to remove water. Then, NaOH (0.5 wt % of CLA) was added under stirring. The vacuum was maintained for another 20 min at 140°C to obtain CLA sodium salt, the catalyzer of the anionic ring-opening polymerization. Then, *N*-COCLA (0.5 wt % of CLA) was added. Immediately, the mixture was poured into a mold preheated to 180°C. After 10 min, the MCPA6/PMMA blends were obtained.

The monomer conversion was measured by the grinding of the dry polymer in a mill at room temperature and then Soxhlet extraction of an accurately weighed sample with hot methanol for 48 h. The extracted samples were dried in a vacuum oven at 150°C for 12 h. They were weighed, and the conversion percentage was calculated as follows:

$$\text{Monomer conversion} = \frac{m_1 - xm_0}{m_0 - xm_0} \times 100\% \qquad (1)$$

where m_1 is the polymer weight after extraction, m_0 is the polymer weight before extraction, and x is the PMMA weight fraction in the blend. The monomer conversions for MCPA6/PMMA blends are shown in Table I.

TABLE I
Monomer Conversion of MCPA6

Sample	PMMA content (wt %)	Conversion (%)
Pure MCPA6	0	96.0
MCPA6 /PMMA	0.5	95.7
	1	91.3
	2	93.2
	5	92.5
	10	87.7

Characterization

DSC measurements were performed on a Netzsch DSC 200 PC (Bavaria, Germany) in a nitrogen atmosphere with a heating and cooling rate of 10 K/min. Calibration was achieved with standard indium samples. All the measurements were performed from room temperature to 250°C with a standstill for 5 min to erase any previous thermal history, and then subsequent cooling and second heating cycles were recorded. The melting enthalpy in the second heating scan was used to measure the degree of crystallization (X_c) according to the following equation:

$$X_c = \Delta H_f / F\Delta H_f^* \times 100\% \qquad (2)$$

where ΔH_f is the melting enthalpy of MCPA6 [or polyamide 6 (PA6)] in the sample, F is the homopolymer weight fraction in the blend, and ΔH_f^* is the melting enthalpy of the matrix polymer at 100% crystallization ($\Delta H_f^* = 230$ J/g).[8] XRD was performed with a Rigaku D/Max-III XRD analyzer (Tokyo, Japan) equipped with a rotating Cu anode generator system using Cu/Kα1 ($\lambda = 1.540$ Å) radiation. XRD data were measured at room temperature. The diffraction angle (2θ) was varied from 5 to 50°. The data were accumulated for 6 s at angular intervals of $2\theta = 0.1°$. Scanning electron microscopy (SEM) was performed on a JSM-5600LV scanning electron microscope (JEOL, Tokyo, Japan) with an accelerated voltage of 15 kV. The process of preparation was as follows: After being fractured in liquid nitrogen, the samples were etched in tetrahydrofuran (THF) for 24 h at the ambient temperature to remove PMMA domains. The etched surfaces were gold-sputtered before examination. Dynamic mechanical properties were measured with a TA Q800 (TA Instruments, New Castle, DE) in the dynamic mechanical analysis multifrequency–strain mode at a frequency of 1 Hz and a heating rate of 2°C/min as a function of temperature from −100 to 150°C.

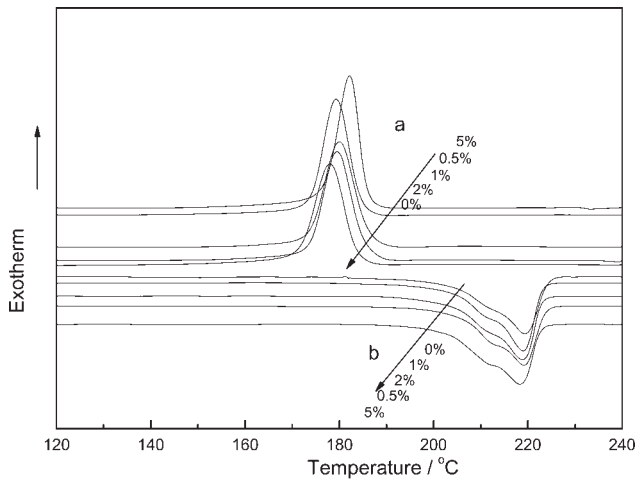

Figure 1 Thermograms of MCPA6/PMMA with various amounts of PMMA: (a) cooling and (b) second heating.

Rheological measurements were carried out on an Advanced Rheometric Expansion System (TA Instrument) with a parallel-plate fixture (25-mm diameter). Dynamic frequency sweep experiments were carried out under a nitrogen flow, the viscosity and storage modulus being measured as functions of the shear rate (ranging from 0.1 to 100 rad/s) at 230°C. The measurements were made with 1-mm-thick samples and a constant shear amplitude of 0.5%. The pore structure was investigated with a Quantachrome Autosorb-1 automatic volumetric sorption analyzer (Boynton Beach, FL) using N_2 as the adsorbate at 77.36 K. The micropore and mesopore volumes were determined with methods described elsewhere.[9] TGA was carried out with a Pyris 1 thermogravimetric analyzer (Perkin-Elmer, Boston, MA) at a heating rate of 20°C/min up to 550°C under a nitrogen flow.

RESULTS AND DISCUSSION

Crystallization behavior of MCPA6/PMMA

The crystallization behavior of the MCPA6/PMMA blends was investigated with DSC. The heating and cooling thermograms of neat MCPA6 and MCPA6/PMMA blends with various PMMA contents are compared in Figure 1. The data are summarized in Table II in detail.

DSC cooling scans of MCPA6 and MCPA6/PMMA blends are shown in Figure 1(a). PMMA had almost no effect on the crystallization temperature of MCPA6. Furthermore, Table II shows that the degree of crystallization of MCPA6 increased versus that of neat MCPA6, and this indicates that the ability to crystallize was improved by the addition of PMMA. In addition, the initial temperature of crystallization in the cooling scan for MCPA6/PMMA with various amounts of PMMA did not significantly shift, and the addition of a small amount of PMMA (0.5 wt %) could also cause a significant increase in the crystallinity degree of MCPA6. This suggests that a small amount of PMMA could act as a heterogeneous nucleation agent for the MCPA6 matrix and enhance its crystallization rate.[10–12]

TABLE II
Characteristic Values of the Crystallization and Melting Behavior of MCPA6/PMMA

Sample	MMA content (wt %)	T_{m1} (°C)	T_{m2}(°C)	T_c (°C)	ΔH_m (J/g)	X_c (%)
Pure MCPA6	0	211.6	218.2	178.0	44.7	19.4
MCPA6/PMMA	0.5	211.6	218.9	179.6	60.0	26.1
	1	211.7	219.4	181.7	55.1	24.0
	2	212.4	218.9	179.3	56.7	24.7
	5	211.7	219.2	182.2	60.6	26.3

ΔH_m = melting enthalpy; T_c = crystallization temperature; T_{m1} = first melting temperature; T_{m2} = second melting temperature; X_c = degree of crystallization.

The second-heating DSC traces are presented in Figure 1(b), in which melting peaks around 211.7 and 218.8°C can be attributed to the melting peaks of the γ-crystalline form and the α-crystalline form, respectively.[13] With the PMMA content increasing, the melting peak of the γ-crystalline form swelled. This is evidence that PMMA chains favor the formation of the γ-crystalline form, and this was also verified with XRD.

Figure 2 displays the XRD patterns of MCPA6/PMMA blends with various amounts of PMMA. Peaks at about 20.1 and 23.8° can be assigned to (200+002) and (002) planes of the α-crystalline form, respectively. The peak around 21.3° is characteristic of (200) and (101) planes of the γ-crystalline form.[13,14] As shown later in Figure 4, the introduction of PMMA greatly changed the crystallization behavior of MCPA6/PMMA. With the PMMA

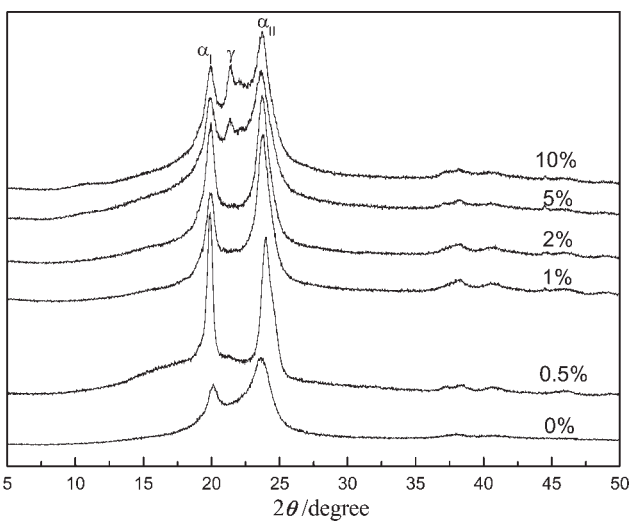

Figure 2 XRD patterns of MCPA6/PMMA with various amounts of PMMA.

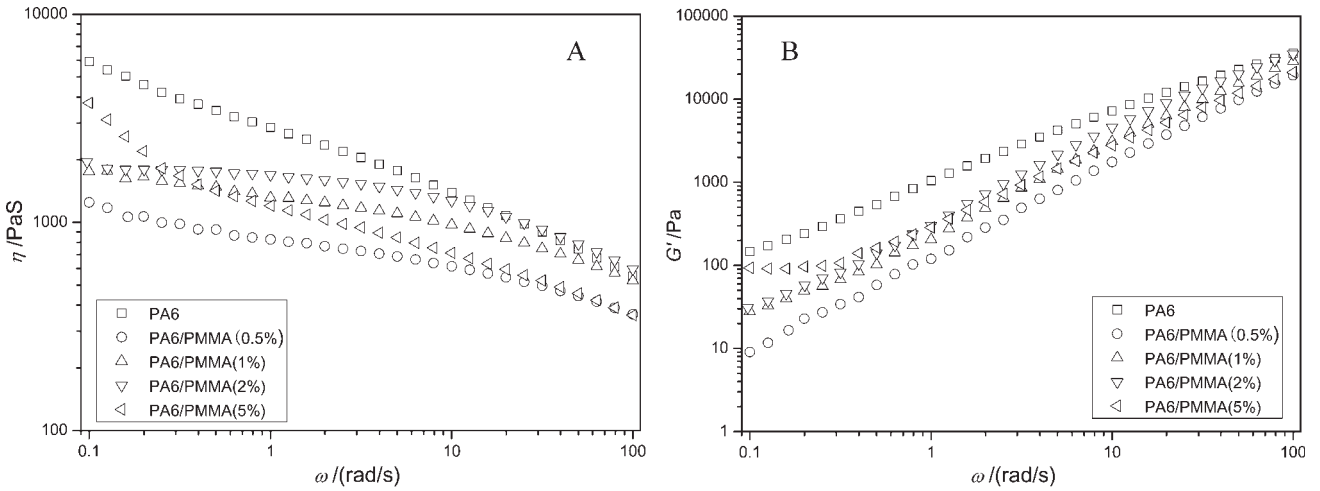

Figure 3 Plots of (A) log η versus log ω and (B) log G' versus log ω at 230°C for MCPA6/PMMA blends (η = viscosity; ω = shear rate; G' = storage modulus).

content increasing, the γ-crystalline form appeared and the α-crystalline form weakened, and this suggests that PMMA chains favor the formation of the γ-crystalline form. This may be due to the fact that in this situation, the phase separation of this polymer pair may start after or simultaneously with the crystallization. Therefore, PMMA chains would act as nucleating centers and restrict the free motion of the MCPA6 molecule chains to form the more stable α-crystalline form.

Rheological behavior of MCPA6/PMMA

The rheological properties of various representative blends were measured and are shown in Figure 3. Comparing the viscoelastic response of MCPA6/PMMA blends with that of pure MCPA6, we can see in Figure 3(A) that the viscosity of the MCPA6/PMMA blends was not higher than that of pure MCPA6 throughout the explored frequency range. This could be due to the fact that the introduction of PMMA with a carbonyl group on its side chains lowered the density of hydrogen bonding and reduced the interaction between MCPA6 chains.

The storage modulus is defined as the stress, in phase with the strain in a sinusoidal deformation, divided by the strain; this is a measure of the energy stored and recovered per cycle for different systems when they are compared at the same strain amplitude.[15] The changes displayed in Figure 3(B) indicate that the storage modulus increased with increasing frequency and that the storage moduli of those blends all had lower values than that of the neat MCPA6. On a molecular basis, the magnitude of the storage modulus depends on what contour rearrangements can take place within the period of the oscillatory deformation. As the frequency increased, the molecular action time became short, and the movement responses of small-dimension units in MCPA6 were dominant. For the blends, segmental relaxation is most likely to be liberated by an interaction between MCPA6 and PMMA, thus leading to a lower storage modulus than that of the pure MCPA6.

Furthermore, the viscosity of MCPA6/PMMA (5 wt %) did not reach a plateau value, and it tended to show leveling off in the storage modulus at low frequencies. This gel-like characteristic[16,17] is due to a network. This could be attributable to the chemical reaction between PMMA and CLA. The carbonyl group on the side chains of PMMA would act as an activator to catalyze anionic ring-opening polymerization. There would also be some ester–amide exchange reaction.[18,19] These two reactions could result in some graft copolymer or some crosslinking. However, MCPA6/PMMA (5 wt %) could be dissolved in sulfuric acid, and the molecular weight of each samples was acceptable. Therefore, the degree of crosslinking was not very high, and this indicates that PMMA has a faint activity activating the anionic ring-opening polymerization of CLA, unlike polyesters with their ester linkages on their bone chains, which could activate the anionic ring-opening polymerization of CLA to achieve block copolymers.

Morphology of the MCPA6/PMMA blends

The morphology of the MCPA6/PMMA blends is shown in Figure 4. PMMA domains were etched with THF. With PMMA contents increasing to 5 wt %, the average size of the PMMA domains increased from approximately 0.5 to 5 μm. The PMMA domains were homogeneously dispersed in the matrix of MCPA6, and the interfaces were smooth. When the content of PMMA reached 10 wt %, PMMA became the continuous phase. Spherulites with interstices were obtained after the removal of PMMA. This indicated that in this situation, the

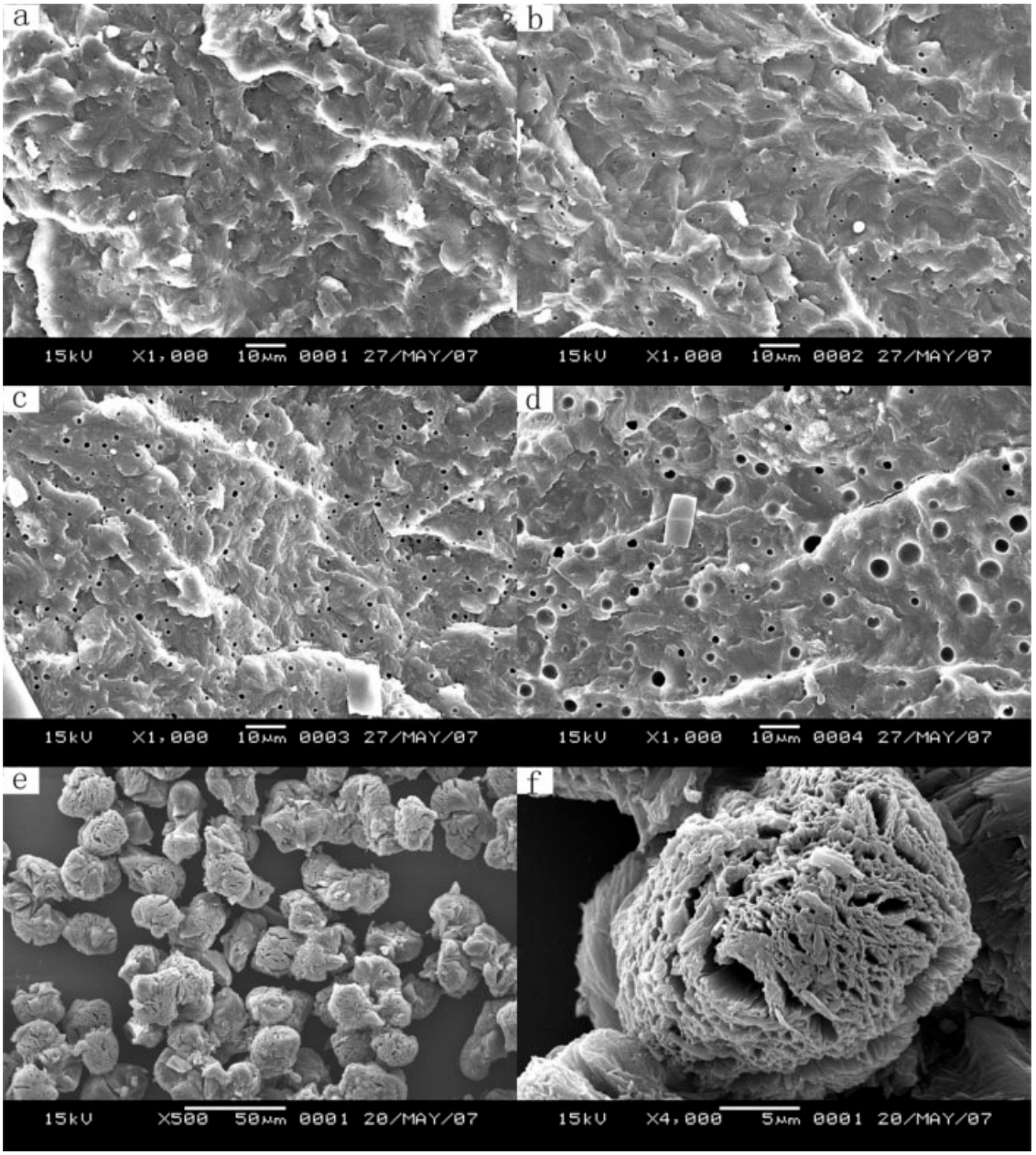

Figure 4 SEM images of MCPA6/PMMA blends: (a) 0.5, (b) 1, (c) 2, and (d) 5 wt % (fractured in liquid nitrogen, the samples were etched in THF for 24 h at the ambient temperature to remove PMMA domains) and (e,f) 10 wt % (the samples were etched in THF for 24 h at the ambient temperature to remove PMMA domains).

relative rates of crystallization and phase separation might be comparable, and the phase separation might start with simultaneous crystallization.[20] Thus, there must be crystallization-induced phase separation. The PMMA phase would be embedded inside the spherulites of MCPA6, and this is in good agreement with Carone et al.'s results[21] and the aforementioned DSC results.

Characterization of the microporous PA6/PMMA particles

As shown in Figure 5, when the content of PMMA reached 10 wt %, microporous particles were obtained after the removal of PMMA domains, the continuous phase. FTIR of the particles showed that there was a small amount of PMMA enclosed in the particles. These PMMA chains could not be removed by THF. Therefore, we used a convenient method to prepare microporous particles: (1) the anionic ring-opening polymerization of CLA in the presence of PMMA with a content of 10 wt %, (2) the removal of the continuous-phase PMMA chains by THF, and (3) filtration and drying. The surface properties and thermal stability of the microporous MCPA6/PMMA particles were studied with BET and TGA, respectively.

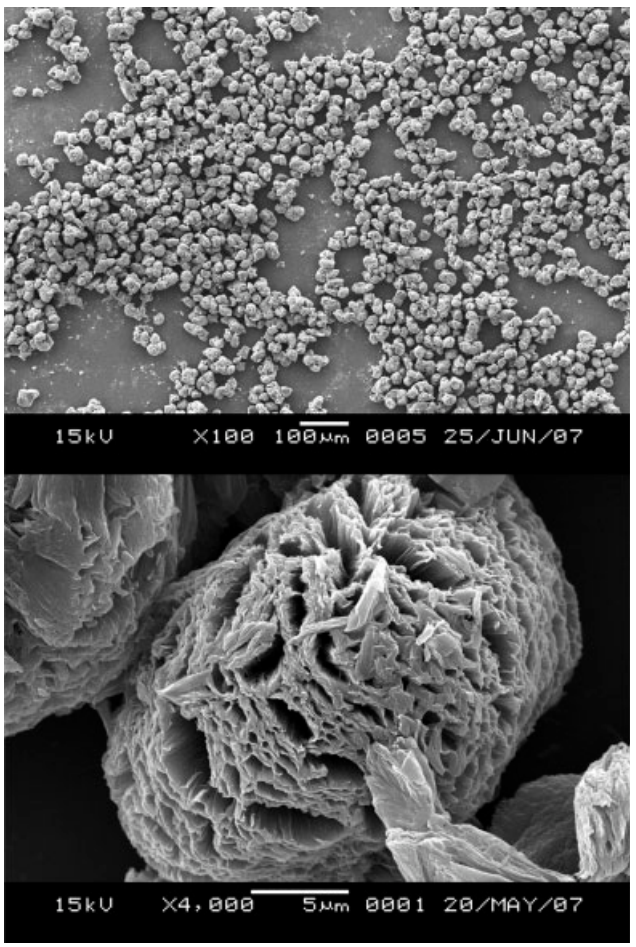

Figure 5 SEM images of microporous MCPA6/PMMA particles.

Figure 6 shows an N_2 adsorption–desorption isotherm of the particles. At relative pressures less than 0.8, the isotherm shows an almost flat sorption characteristic. Furthermore, there is almost no hysteresis loop in the isotherm. The surface area of the microporous particles and pore volume were calculated from this isotherm to be 3.14 m^2/g and 0.013 cm^3/g, respectively.

Figure 7 shows typical TGA weight-loss and derivative thermograms [derivative thermogravimetry (DTG)] for MCPA6 and PA6/PMMA particles in a nitrogen environment. The TGA 10, 30, and 50 wt % loss temperatures ($T_{10\ wt\ \%}$, $T_{30\ wt\ \%}$, and $T_{50\ wt\ \%}$, respectively), maximum decomposition temperature (T_{max}), and char yield are summarized in Table III. It is known from literature data related to the thermal degradation of the polyamides that chain scission takes place at the —NH—CO— bonds in the neighborhood of the carbonyl group.[22–24] $T_{10\ wt\ \%}$, $T_{30\ wt\ \%}$, $T_{50\ wt\ \%}$, and T_{max} of the MCPA6/PMMA particles were reduced in comparison with those of the neat MCPA6. The MCPA6/PMMA particles had poorer thermal stability than MCPA6, and this probably can be attributed to the fact that a powder material with a larger surface area has poor thermal stability than one in bulk or in the presence of a slight amount of PMMA, which has poor thermal stability and might accelerate the thermal degradation of MCPA6.

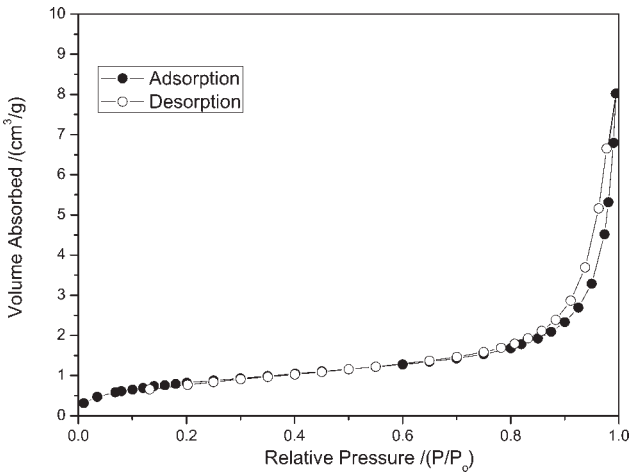

Figure 6 N_2 adsorption–desorption isotherms for microporous MCPA6/PMMA particles at 77.39 K.

CONCLUSIONS

We successfully synthesized MCPA6/PMMA blends by continuous synthesis in two steps: (1) radical polymerization of methyl methacrylate in CLA and (2) anionic ring-opening polymerization of CLA. The DSC and XRD results showed that PMMA could act as a heterogeneous nucleation agent and favored the formation of the γ-crystalline form. The rheological and dynamic mechanical analysis results indicated that PMMA reduced the interaction between MCPA6 chains by lowering the density of hydrogen bonding. We also used a novel and convenient

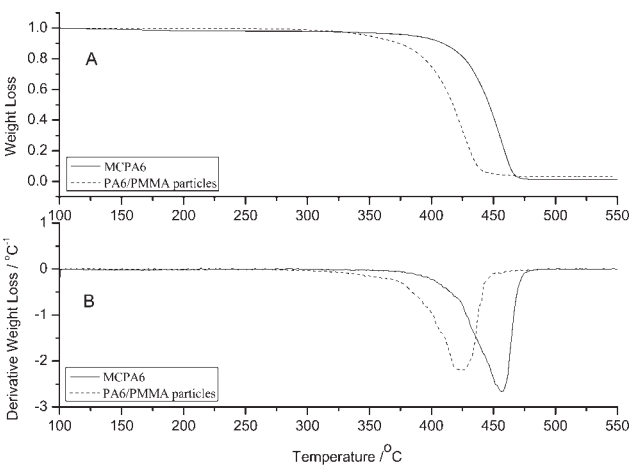

Figure 7 (A) TGA and (B) DTG curves of MCPA6 and MCPA6/PMMA particles.

TABLE III
$T_{10\ wt\ \%}$, $T_{30\ wt\ \%}$, $T_{50\ wt\ \%}$, Char Yield, and T_{max} Values for MCPA6 and Microporous MCPA6/PMMA Particles

Sample	$T_{10\ wt\ \%}$ (°C)	$T_{30\ wt\ \%}$ (°C)	$T_{50\ wt\ \%}$ (°C)	Char yield (%)	T_{max} (°C)
MCPA6 in bulk	409.4	435.1	446.6	1.2	454.3
MCPA6/PMMA particles	356.3	390.7	413.2	3.1	416.7

method to prepare microporous PA6/PMMA particles. A continuous phase of PMMA was carried out with 10 wt % PMMA, and the interface between the dispersive MCPA6 phase and the matrix of PMMA was porous; this indicated crystallization-induced phase separation. The PMMA phase was embedded inside the spherulites of MCPA6. Microporous PA6/PMMA particles with a larger surface area were obtained through the removal of the continuous phase. The surface area of the microporous particles and pore volume were calculated by the BET method to be 3.14 m^2/g and 0.013 cm^3/g, respectively. TGA results showed poorer thermal stability compared with that of MCPA6 in bulk.

References

1. Ji, Y.; Ma, J.; Liang, B. Polym Bull 2005, 54, 109.
2. Stehlıcek, J.; Sebenda, J.; Wichterle, O. Chem Commun 1964, 29, 1236.
3. Merna, J.; Chromcova, D.; Brožek, J.; Roda, J. Eur Polym J 2006, 42, 1569.
4. Draye, A. C.; Persenaire, J.; Brozek, J.; Roda, J. Polymer 2001, 42, 8325.
5. Werner, R. A.; Hayes, B. H. U.S. Pat. 3,758,631 (1973).
6. Merna, J.; Chromcova, D.; Brožek, J.; Roda, J. Polymer 2004, 45, 2141.
7. Hou, L.; Liu, H.; Yang, G. Polym Eng Sci 2006, 46, 1196.
8. Evstatiev, M.; Schultz, J. M.; Petrovich, S.; Georgiev, G.; Fakiov, S.; Friedrich, K. J Appl Polym Sci 1998, 67, 723.
9. Kyotani, T.; Nagai, T.; Inoue, S.; Tomita, A. Chem Mater 1997, 9, 609.
10. Run, M.; Wub, S.; Zhang, D.; Wu, G. Polymer 2005, 46, 5308.
11. Rusu, G.; Rusu, E. High Perform Polym 2006, 18, 355.
12. Cho, J. W.; Paul, D. R. Polymer 2001, 42, 1083.
13. Kyotani, M.; Mitsuhashi, S. J Polym Sci Part A-2: Polym Phys 1972, 10, 1497.
14. Coppola, G.; Pallesi, B. Polymer 1974, 15, 130.
15. Ferry, J. D. Viscoelastic Properties of Polymers; Wiley: New York, 1970.
16. Tol, R. T.; Groeninckx, G.; Vinckier, I.; Moldenaers, P.; Mewis, J. Polymer 2004, 45, 2587.
17. Okada, A.; Kawasumi, M.; Tajima, I.; Kurauchi, T.; Kamigaito, O. J Appl Polym Sci 1989, 37, 1363.
18. Kimura, M.; Porter, R. J Polym Sci Polym Phys Ed 1983, 21, 367.
19. Pillon, L.; Utrack, L. A. Polym Process Eng 1986, 4, 375.
20. Hong, P. D.; Huang, H. T.; Chou, C. M. Polym Int 2000, 49, 407.
21. Carone, E., Jr.; Felisberti, M. I.; Pereira, S. J Mater Sci 1998, 33, 3729.
22. Rusu, G.; Rusu, E. High Perform Polym 2004, 16, 569.
23. Kondelkova, J.; Tuzar, Z.; Kraliceck, J.; Sandova, K.; Strohalmova, M.; Kubanek, V. Angew Macromol Chem 1977, 64, 123.
24. de la Campa, J. G.; Guijarro, E.; Serna, F. J.; de Abajo, J. Eur Polym J 1985, 21, 1013.